

Study of Structural, Morphological and Optical Properties of Nano-Structured Zinc doped V_2O_5 Thin Films

T. Akkila^{1,*} and I. Mansur Basha²

^{1,*}PG& Research Department of Physics, Govt. Arts College, Trichy, Tamilnadu, India.

²PG& Research Department of Physics, Jamal Mohamed College (Autonomous), Trichy, Tamilnadu, India.

Thin films of zinc-doped vanadium pentoxide with different Zn doping levels (in steps of 0.1mM of Zn) were deposited on glass substrates by a home built spray pyrolysis system. The effect of Zn doping on the structural, morphological and optical characteristics were carried out. X-ray diffraction (XRD) patterns revealed that prepared films were polycrystalline in nature, having an orthorhombic crystal structure. Annealing effect improved the crystallinity of the films. The crystallite size of the films was found to increase after annealing. From the FESEM image, the rod shape was observed in the annealed pristine V_2O_5 film. The band gap energies of as deposited and annealed pristine V_2O_5 film were 2.16eV and 2.18eV respectively. The band gap energy of as deposited films varied with Zn doping.

Keywords: Thin films, Zinc Doping, Spray pyrolysis, X-ray diffraction.

1. INTRODUCTION

Amidst different metal oxides, synthesis of vanadium oxide thin films at low temperature has become a challenging one. Specifically, V_2O_5 films have attracted much interest due to their distinctive features such as multi valency, layered structure, wide optical band gap, good chemical and thermal stability and excellent thermoelectric properties [1]. These features suggest V_2O_5 as a potential material for gas sensing applications [2], thin film battery [3], optical-electrical switches [4] and smart windows [5].

Synthesis of doped nanostructured V_2O_5 for wide applications has recently been the subject of much research. It has been revealed that the properties of V_2O_5 could be upgraded by introducing various metal ions into host lattice. Hence many attempts were made such as Ag [6], Mo [7], Sn [8], Zr [9], Na [10], F [11], Cu [12], Zn [13] and Cr [14] in order to enhance the electrochemical, electrochromic and thermoelectric properties by various methods.

Though several sophisticated methods are available, spray pyrolysis is a modest and inexpensive method. It is used for large area depositions with good uniformity and porosity in films [15] and yields oxide films of high quality at rather low costs when properly controlled. This method offers a list of controlling parameters such as solution molarity, substrate temperature, annealing temperature, annealing time and dopant effects. Particle formation mainly depends on the shape of the droplet sprayed on preheated substrate. Hence the formations of clusters initially are avoided. The size of the droplets can be monitored at the nanoscale at low temperatures [16]. Spray pyrolysis is not limited to specific metal oxide and is widely used to prepare various metal oxides.

Zn as a dopant in VO_2 has been studied by dc reactive magnetron sputtering [11]. Zinc (Zn) is an important transition metal element having an ionic radius of 0.074 nm, which is slightly greater than that of V^{5+} (0.059nm) and hence Zn^{2+} ions can possibly incorporate into the V_2O_5 crystal lattice and substitute partially V^{5+} position in the crystal. By this process of doping a low valence cation into V_2O_5 lattice, one can modify the growth kinetics considerably. In the present work, we have studied the doping and post annealing effects of Zn in V_2O_5 at different concentrations of Zn and have reported the structural, morphological and optical properties of the prepared samples.

2. EXPERIMENTAL

2.1. Preparation of Zn-Doped V_2O_5 Thin Films

Vanadium (III) chloride (Sigma-Aldrich, USA, purity 99.8%) and Zinc chloride, (Sigma-Aldrich, USA, purity 99.8%) were used as sources of vanadium and zinc oxides respectively. Firstly, for pristine V_2O_5 thin film 0.05M of vanadium (III) chloride (VCl_3) was dissolved in 50 mL of deionized water. For Zn doped V_2O_5 , an appropriate quantity of Zinc chloride ($ZnCl_2$) was added from 0.1mM to 0.5mM in steps of 0.1mM in the precursor solution respectively. The solution was stirred thoroughly using a magnetic stirrer for 30 min and then deposited on the preheated glass substrates kept at 250°C by spray pyrolysis system. A home built spray system was constructed as reported by Jeyaparakash *et. al.* [17].

Before the deposition process, the glass substrates were cleaned chemically and dried to remove the unwanted organic matters present in the substrate. The cleaned glass substrates were placed on the heater which is controlled by chrome-nickel thermocouple fed to a temperature controller with an accuracy of $\pm 1^\circ C$. The solution was sprayed at an angle of 45° onto preheated glass substrate kept at a distance of 50cm from the spray gun. Compressed dry air at a pressure of 2 kg/cm² by an air compressor via an air filter with regulator was employed as the carrier gas and spray rate of the solution was kept at 3 ml/min. To avoid excessive cooling of substrates, consecutive spraying process was employed with the time period of 15 seconds between two sprays. All the prepared film samples were post annealed at 300°C for 1 hour in an air atmosphere.

2.2. Characterization Techniques

The structural details of the thin films prepared by the afore mentioned process, were carried out by P Analytical X-ray diffractometer (Model D/MAX ULTIMA III) using Ni-filtered Cu K(alpha) X-radiation ($k=1.54056\text{\AA}$). A range of 2θ from 10° to 100° was scanned from a fixed slit type so that all possible diffraction peaks could be detected. Crystallite size and micro strain were analyzed by X-Ray line broadening technique. Surface morphology of the films was investigated using Field Emission Scanning Electron Microscope (Model Carl Zeiss Ultra 55) with an accelerating potential of 18KV. Prior to the imaging, the films were sputtered with a thin gold film to increase the emission of the secondary electron for enhanced imaging. All the spectra were acquired at a pressure using an ultra-high vacuum with Al Ka excitation at 250W. The optical properties and the band gap of the thin films were analyzed by UV-VIS-NIR spectrophotometer (Model- Lambda 35).

3. RESULTS AND DISCUSSION

3.1. Structural Analysis

Figure 1 shows the XRD patterns of as deposited pristine and Zn doped vanadium pentoxide thin films. As seen, all the as deposited films are polycrystalline in nature. The peaks observed in pristine V_2O_5 film at $2\theta = 15.4^\circ, 20.2^\circ, 26.1^\circ, 31.0^\circ, 32.4^\circ, 41.1^\circ, 47.3^\circ$ and 51.1° correspond to (2 0 0), (0 0 1), (1 1 0), (3 0 1), (3 1 0), (0 0 2), (6 0 1) and (0 2 0) planes respectively. It confirms the typical V_2O_5 orthorhombic phase [JCPDS Card No. 41- 1426] with lattice parameter values of $a = 11.516$, $b = 3.5656$ and $c = 4.3727$ Å. The observed pattern is in accordance with the other V_2O_5 films prepared by the spray pyrolysis and other methods [18-20]. Films doped with 0.3mM and 0.4mM of Zn has a V_4O_9 phase with preferred orientation along (1 0 1) and (4 0 1) planes (JCPDS Card: 24-1391, 23-0720). For all the pristine and Zn doped films (0 0 1) peak is predominant. But the intensity of (0 0 1) was found to be decreased with an increase in the dopant concentration due to smaller crystallite size. Moreover, the doping of Zn^{2+} ions in the V-O lattice deteriorates V_2O_5 phase. A film with 0.5mM of Zn doping was found to be amorphous in nature due to the accumulation of Zn on the grain boundaries of host V-O lattice.

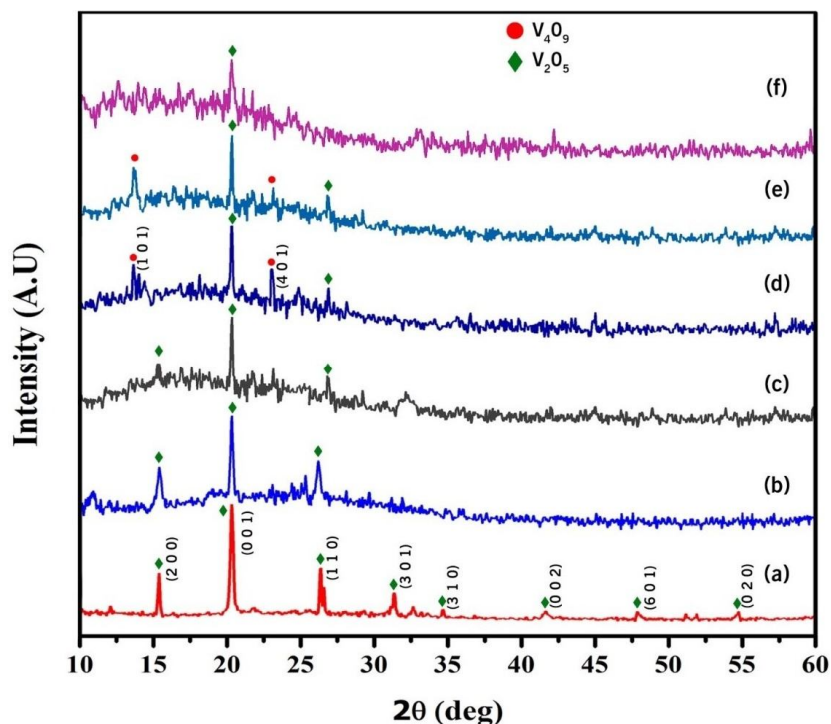


Fig. 1: XRD patterns of as deposited (a) Pristine V_2O_5 and Zn doped (b) 0.01 mM (c) 0.02 mM (d) 0.03 mM (e) 0.04 mM (f) 0.05 mM, V_2O_5 thin films

Figure 2 shows the XRD patterns of annealed pristine and Zn - doped vanadium pentoxide thin films. The observed peaks indicated that all the films have polycrystalline nature. Pristine V_2O_5 film showing an improved crystallinity at diffraction angle of 12.8°

indicates β - V₂O₅ phase with tetragonal structure and having a preferential orientation along (2 0 0) plane [JCPDS Card No. 45-1074]. A change of phase from V₂O₅ to β -V₂O₅ after annealing was observed by many other researchers [21–23]. In the case of Zn doped films, the growth was stabilized with reference to as deposited films. It might be due to the enrichment of dopant mobility resulting in an improvement in the quality and crystallinity of films. In the case of a film with 0.5mM concentration of Zn, the growth was suppressed with reference to lower doping concentration. It is concluded that excess amount of doping Zn influences growth orientation and hence the morphology of the film [24].

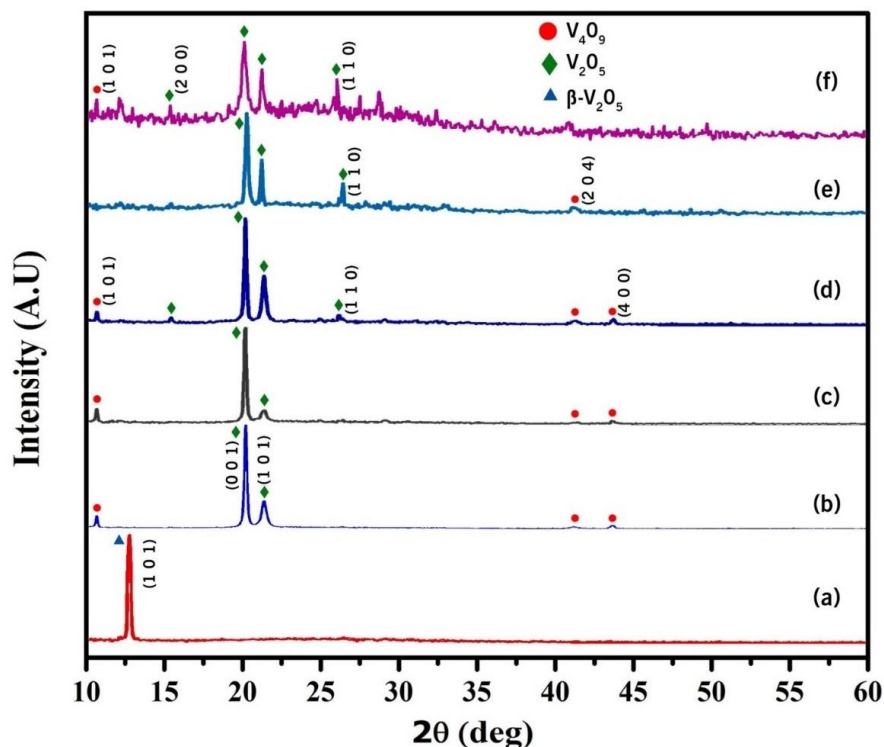


Fig. 2: XRD patterns of annealed (a) Pristine V₂O₅ and Zn doped (b) 0.01 mM (c) 0.02 mM (d) 0.03 mM (e) 0.04 mM (f) 0.05 mM, V₂O₅ thin films

The crystallite size and microstrain were calculated using Scherrer's formula [25],

$$D = 0.9\lambda / \beta \cos\theta \quad (1)$$

$$\text{And } \epsilon_{hkl} = \beta / 4 \tan\theta \quad (2)$$

Where D is the size of the grain in the direction perpendicular to the reflecting planes, θ is diffraction angle, K is shape factor (=0.9), λ is the wavelength of X-ray, β is the full width at half maximum of prominent peaks in radian and ϵ_{hkl} is microstrain. Figure 3(a)

and 3(b) show the variation of mean crystallite size and microstrain for both as deposited and annealed films.

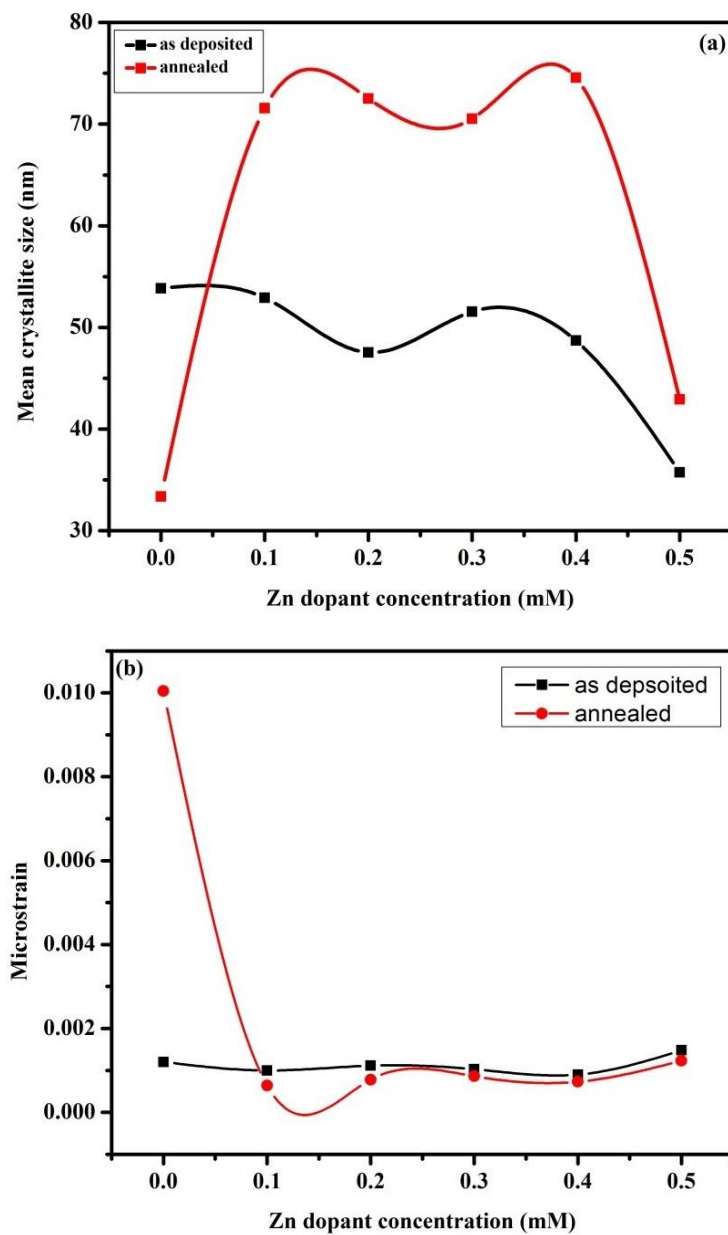


Figure 3: Variation of (a) Mean crystallite size and (b) microstrain of as deposited and annealed pristine and Zn doped V_2O_5 thin films.

It can be seen that crystallite size of pristine V₂O₅ film is found to decrease after annealing with significant phase change. The increase in the dopant concentration decreases the mean crystallite size. This fact is attributed to increasing crystallographic imperfections and lattice disorder, triggered by dopant concentration. After annealing, the crystallite size was found to increase due to coalescence process [26].

Table 1: Variation of structural and optical properties.

Zn dopant concentration (mM)	Mean crystallite size (nm)		Micro Strain ($\times 10^{-3}$)		Band gap energy (eV)	
	As deposited	annealed	As deposited	annealed	As deposited	annealed
0	53.84	33.36	1.20	10.04	2.16	2.18
0.1	52.91	71.57	1.00	0.64	2.36	1.88
0.2	47.55	72.53	1.11	0.78	1.56	1.32
0.3	51.55	70.53	1.03	0.86	2.00	1.48
0.4	48.7	74.57	0.90	0.73	2.24	1.96
0.5	35.73	42.92	1.48	1.23	2.28	1.76

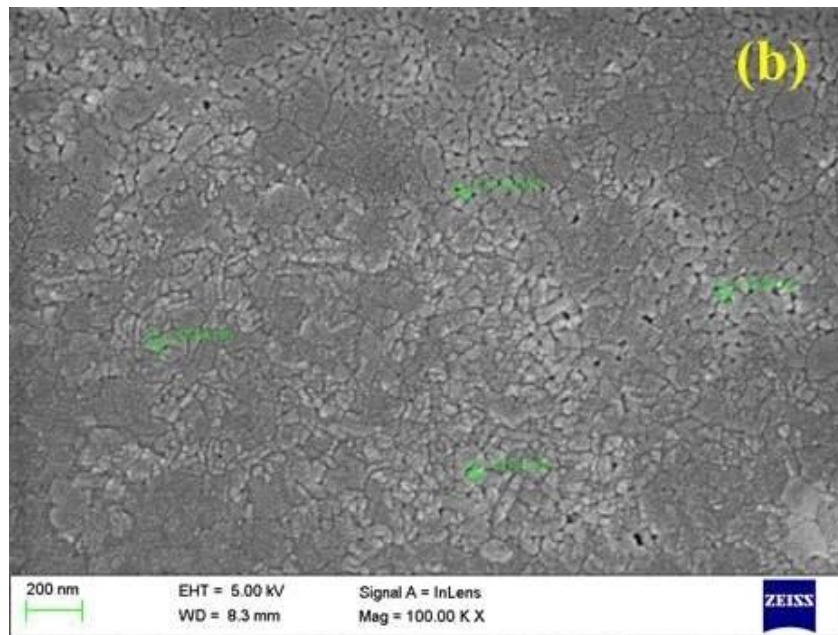
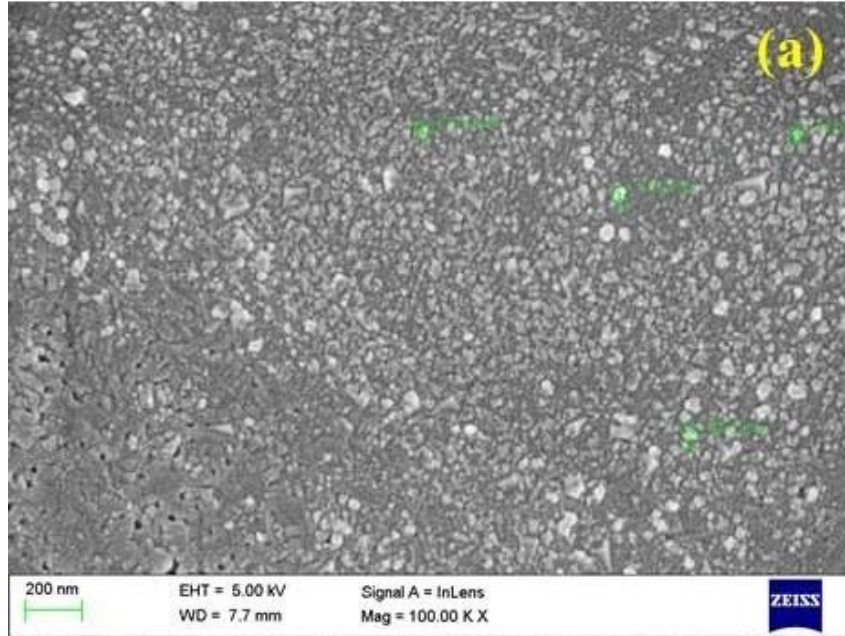
The microstrain was found to increase for the pristine V₂O₅ film after annealing. Annealing temperature increases the internal stress which increases the microstrain [27]. For Zn doped films, the microstrain decreases with annealing. The mobility of Zn²⁺ enhances during annealing. This enhancement may reduce the microstrain and therefore vary the surface morphology. Zn²⁺ ions partially substituted the V⁵⁺ ions and have not formed any Zinc oxide phase.

3.2. Morphological Analysis

The surface morphology of the as deposited and annealed films was studied using FESEM images shown in Figure 4, 5 and 6. In Figure 4, there is a significant change in morphology of the Zn doped films as Zn concentration was increased (Figure 4). The micrographs of as deposited pristine V₂O₅ films depict the featureless, smooth and compact surface with fine pores. Figure 4(b) and 4(c) show different morphology when compared to pristine films. The distortion of the typical V₂O₅ phase with the incorporation of Zn is evidently seen through the FESEM images. As the dopant concentration increased to 0.3mM of Zn, the film surface becomes disordered due to a mixed phase of V₂O₅ and V₄O₉. It clearly shows film doped with 0.5mM of Zn is slightly amorphous in nature and is in confirmation with above mentioned XRD data.

As observed in Figure 5, there is a marked difference between as deposited and annealed films. While annealing the agglomeration process is initiated resulting in the formation of larger grains. In contrast to the as deposited pristine V₂O₅ film, the annealed V₂O₅ film presents a slightly coherent and homogeneous morphology, consisting of rod shaped nano structure which is approximately 300 nm wide as shown in Figure 6. It might be related to the formation of a new phase as depicted in XRD pattern. This type

of rod shaped nanostructure was also observed in pristine V_2O_5 thin films prepared at 500°C substrate temperature using spray technique by Irani *et. al.* [18].



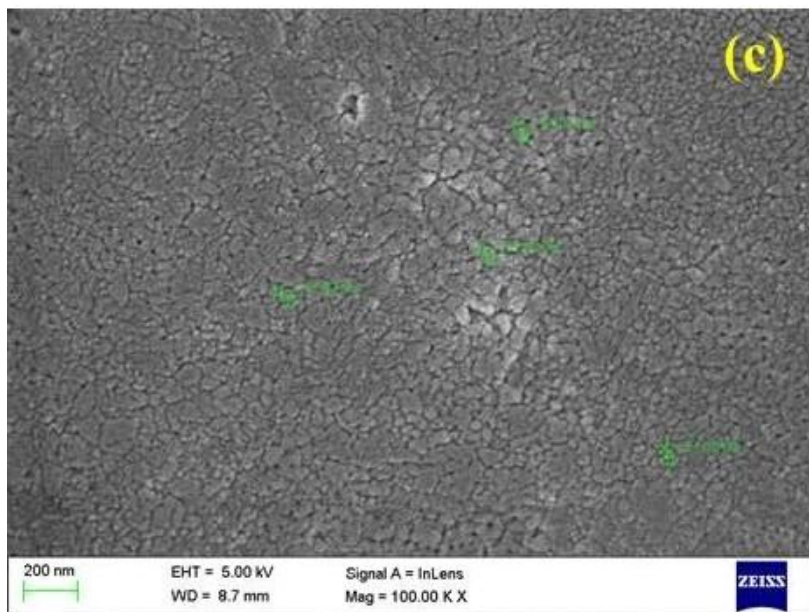
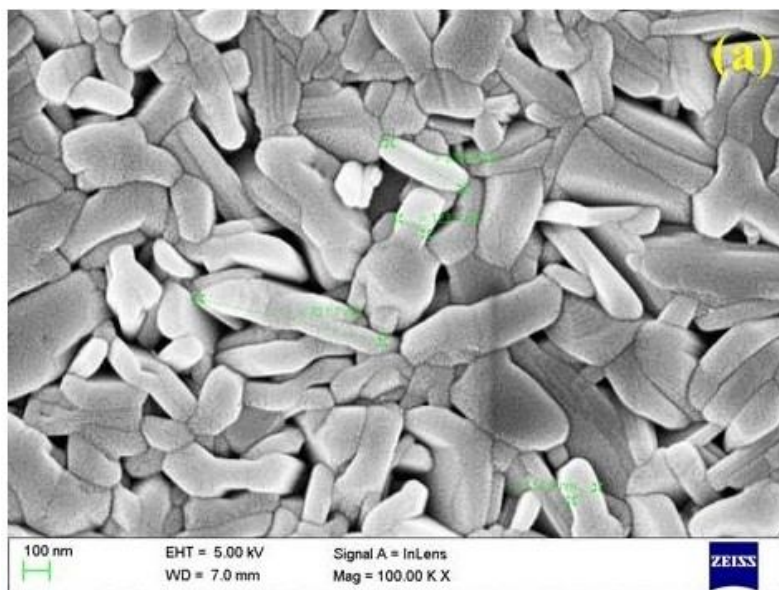


Fig. 4: FESEM images of as deposited (a) and Zn doped with (b) 0.3mM and (c) 0.5mM.

After annealing of Zn doped thin films, densely packed grains transformed into clusters forming larger grains with an irregular shape. It also confirmed that doping with Zn distorted the morphology of the films which was evidently seen in XRD patterns.



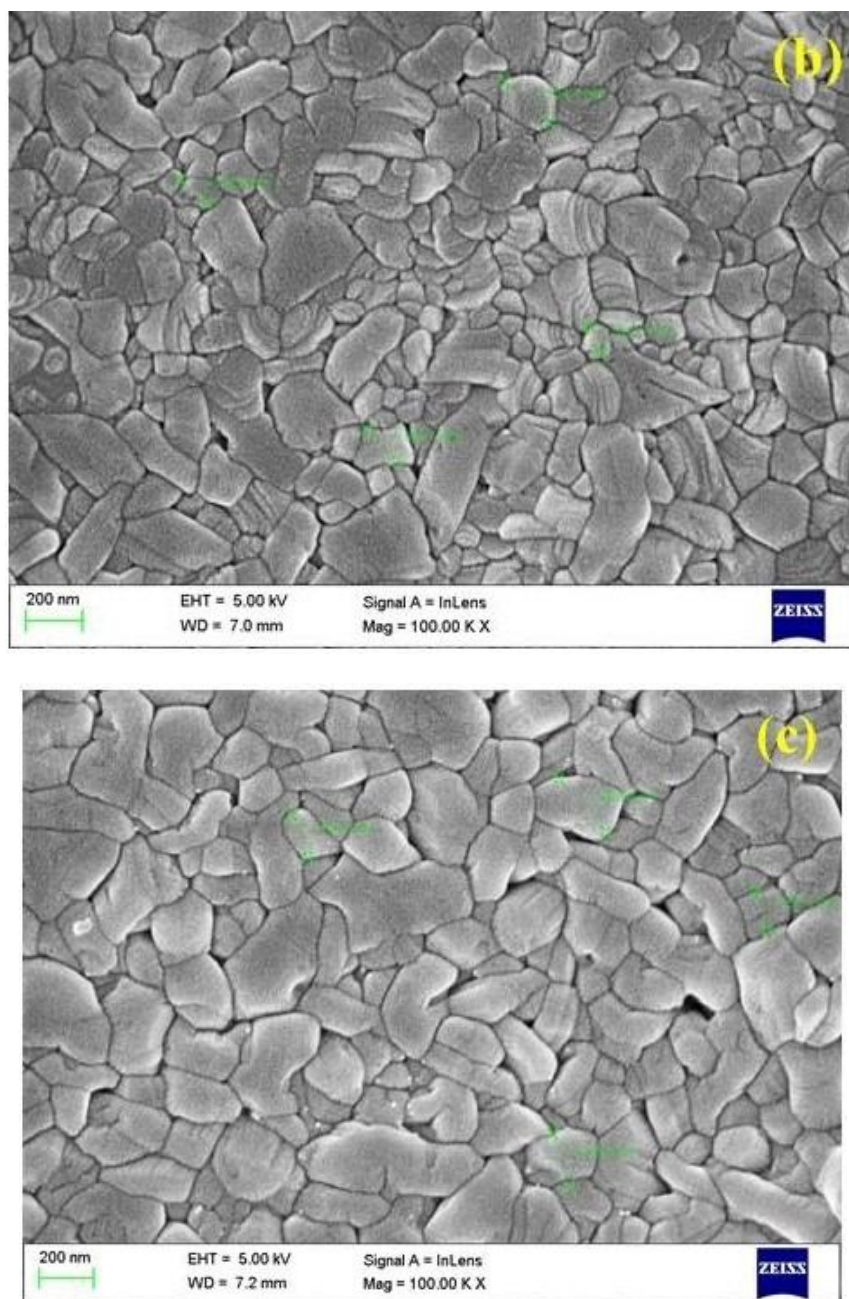


Figure 5: FESEM images of annealed (a) and Zn doped with (b) 0.3mM and (c) 0.5mM.

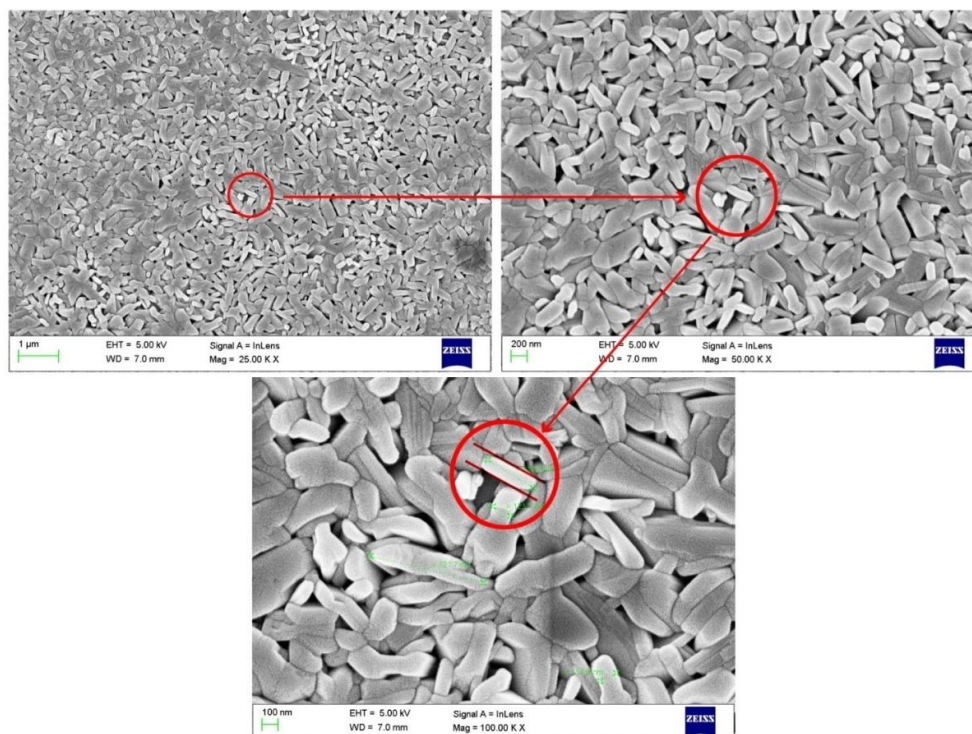


Fig. 6: FESEM images of annealed pristine V₂O₅ thin films with different magnifications of 25k ×, 50k × and 100k ×

3.3. Optical Studies

Figure 7 and 8 show the optical absorption spectra and Tauc's plot of as deposited and annealed pristine V₂O₅ and Zn-doped V₂O₅ thin films. Generally, by increasing the dopant concentration, the optical absorbance decreases intensely. In Figure 7(a), as deposited films doped with 0.3mM and 0.4mM of Zn concentration showed high absorption value. The trend is reversed for low concentration of Zn (0.1mM and 0.2mM). On the other hand, notably film doped with 0.5mM of Zn show lower absorption. It can be stated that the large porosity in 10% of Zn doped film observed in FESEM images, can reduce the refractive index of the film, resulting in a decrease in absorption of the film [28]. The absorbance increased considerably with post annealing at 300°C. The annealed pristine V₂O₅ film showed a high absorbance which indicated the film formation with better crystalline nature.

The optical absorption coefficient ' α ' was estimated as

$$\alpha = 2.303A / t \quad (3)$$

Where A is the absorbance and t is the thickness of the film. The optical band gap was calculated using Tauc's relation given in following equation [29] as

$$(\alpha h\nu)^{1/n} = B (h\nu - E_g) \quad (4)$$

Where $h\nu$ is the photon energy, E_g is the optical band gap of the film, α is the absorption coefficient, 'B' is constant, the exponent 'n' corresponding to the type of transition. The values of n are 1/2, 2, 3/2 and 3, correspond to the allowed indirect, direct, forbidden indirect and forbidden direct band gaps respectively.

In Figure 7(a), as deposited films doped with 0.3mM and 0.4mM of Zn concentration showed high absorption value. The trend is reversed for low concentration of Zn (0.1mM and 0.2mM). The E_g values determined are found to vary from 1.32eV to 2.36eV as shown in Table 1. The optical band gap energies of as-deposited and annealed pristine V_2O_5 are 2.16eV and 2.18 eV respectively which are in agreement with the previous results [30, 31]. In the case of Zn doped films, the band gap energies are decreased after annealing. The variations of E_g with Zn doping concentration of both as deposited and annealed films are shown in Figure 9.

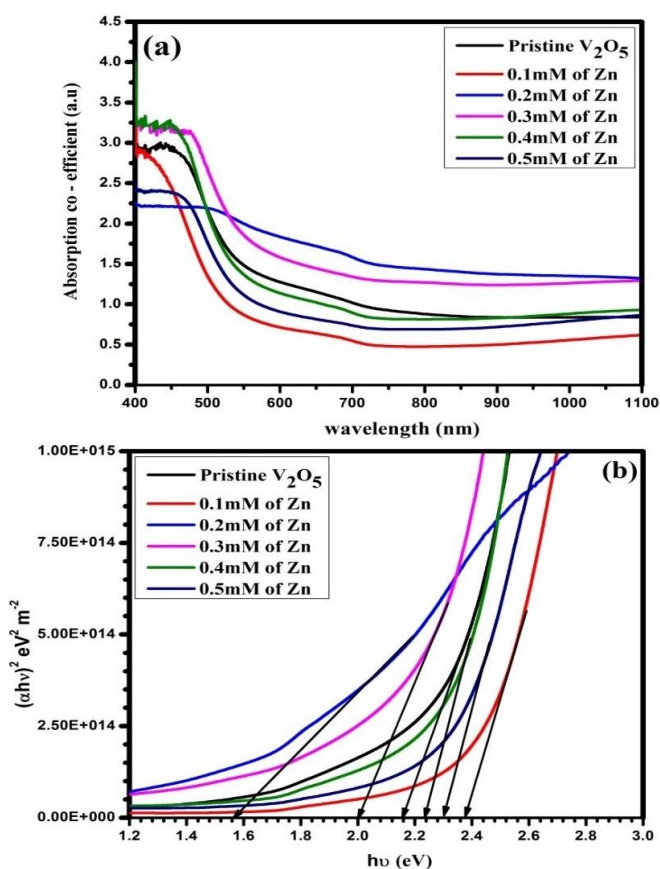


Figure 7: (a) Absorbance spectra and (b) Tauc's plot of as deposited V_2O_5 thin films doped with different Zn concentrations.

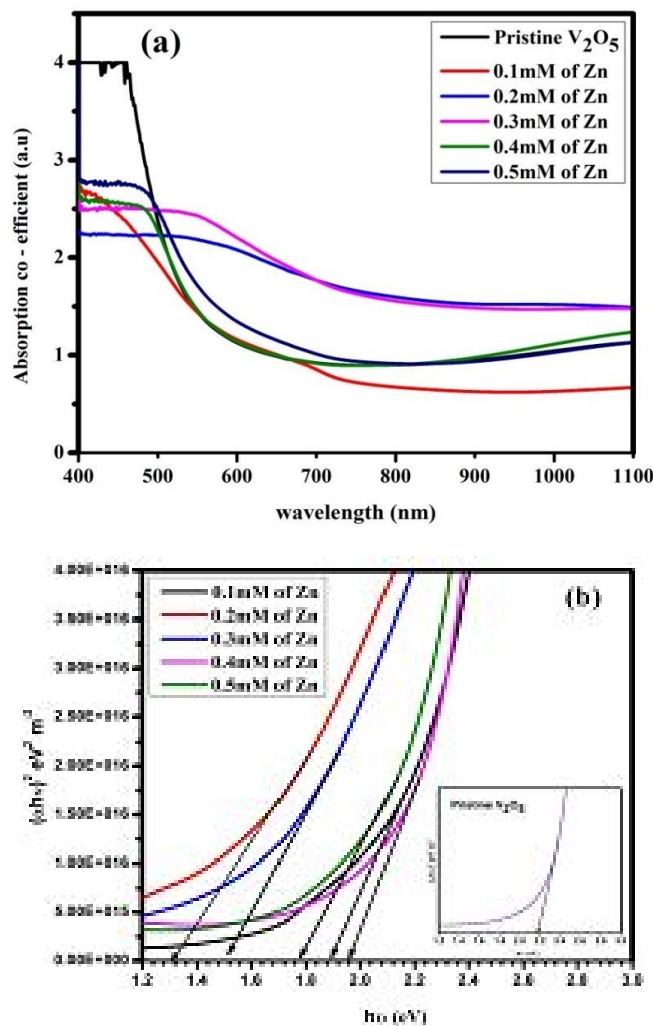


Figure 8: (a) Absorbance spectra and (b) Tauc's plot of annealed V_2O_5 thin films doped with different Zn concentrations.

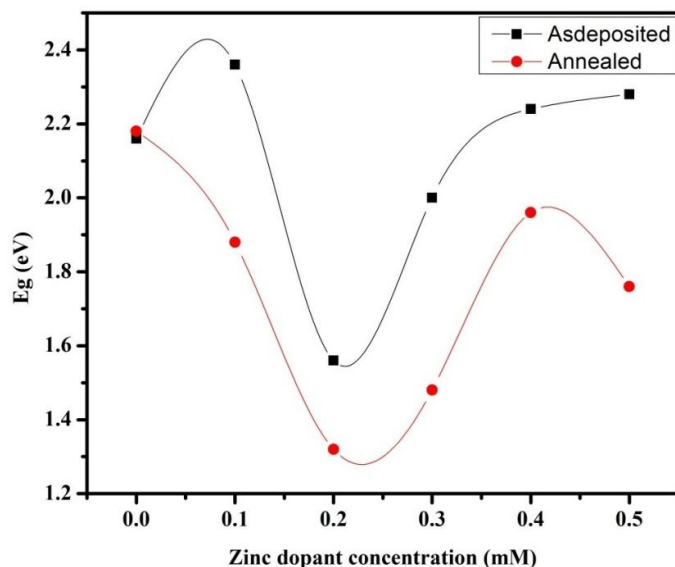


Fig. 9: The variation of E_g with Zn doping concentration.

4. CONCLUSION

The results of the study of structural, morphological, XPS and optical studies of Zn-doped V_2O_5 thin films prepared on glass substrates by a spray pyrolysis technique are reported here. XRD measurements revealed that all the films show polycrystalline nature with a slight variation of phase due to the substitution of V^{5+} by Zn^{2+} ions. Annealed films exhibit improved crystallinity with as deposited films. The crystallite size is increased with annealing whereas the microstrain decreased. The rod shaped nanostructure is observed in annealed pristine V_2O_5 films. The surface roughness of all the prepared films increased with annealing. The band gap of V_2O_5 was tuned upon Zn doping upto 0.5mM. On annealing, the band gap shifts to lower energy. This narrow bandgap energy might be used for detection and generation of infrared radiation and narrow band gap semiconductors.

REFERENCES

- [1] P. Chatterjee, S.P.S. Gupta and S. Sen; "Particle fracture and plastic deformation in vanadium pentoxide powders induced by high energy vibrational ball-mill", Bull. Mater. Sci., Vol. 24(2), pp. 173–180, 2001.
- [2] H. Meixner, J. Gerblinger, U. Lampe and M. Fleischer; "Thin-film gas sensors based on semiconducting metal oxides", Sens. Actuators, Vol. 23(2-3), pp. 119–125, 1995.
- [3] N.J. Dudney, J.B. Bates, R.A. Zuhr, S. Young, J.D. Robertson, H.P. Jun and S.A. Hackney; "Nanocrystalline $Li_xMn_{2-y}O_4$ cathodes for solid state thin-film rechargeable lithium batteries", J. Electrochem. Soc., Vol. 146, pp. 2455-2464, 1999.

- [4] X. Wu, F. Lai, L. Lin, Y. Li, L. Lin, Y. Qu and Z. Huang; "Influence of thermal cycling on structural, optical and electrical properties of vanadium oxide thin films", *Appl. Surf. Sci.*, Vol. 255(5), pp. 2840–2844, 2008.
- [5] Z. Chen, Y. Gao, L. Kang, J. Du, Z. Zhang, H. Luo, H. Miao and G. Tan; "VO₂-based double-layered films for smart windows: Optical design, all-solution preparation and improved properties", *Sol. Energy Mater. Sol. Cells*, Vol. 95(9), pp. 2677–2684, 2011.
- [6] H.S. Hwang, S.H. Oh, H.S. Kim, W.I. Cho, B.W. Cho and D.Y. Lee; "Characterization of Ag-doped vanadium oxide ($Ag_xV_2O_5$) thin film for cathode of thin film battery", *Electrochim. Acta*, Vol.50(2), pp. 485–489, 2004.
- [7] A. Jin, W. Chen, Q. Zhu, Y. Yang, V.L. Volkov and G.S. Zakhharova; "Structural and electrochromic properties of molybdenum doped vanadium pentoxide thin films by sol-gel and hydrothermal synthesis", *Thin Solid Films*, Vol. 517(6), pp. 2023–2028, 2009.
- [8] Y. Li, J. Yao, E. Uchaker, M. Zhang, J. Tian, X. Liu and G. Cao; "Sn-Doped V_2O_5 film with enhanced lithium-ion storage performance", *J. Phys. Chem. C*, Vol. 117(45), pp. 23507–23514, 2013.
- [9] H. Zhang, Z. Wu, X. Wu, X. Wei and Y. Jiang; "Preparation and phase transition properties of nanostructured zirconium-doped vanadium oxide films by reactive magnetron sputtering", *Thin Solid Films*, Vol. 568, pp. 63–69, 2014.
- [10] M.M. El-Desoky, M.S. Al-Assiri and A.A. Bahgat; "Structural and thermoelectric power properties of Na-doped $V_2O_5 \cdot nH_2O$ nanocrystalline thin films", *J. Phys. Chem. Solids*, Vol. 75(8), pp. 992–997, 2014.
- [11] M. Abyazisani, M.M. Bagheri-Mohagheghi and M.R. Benam; "Study of structural and optical properties of nanostructured V_2O_5 thin films doped with fluorine", *Mat. Sci. Semicon. Proc.*, Vol. 31, pp. 693–699, 2015.
- [12] H. Yu, X. Rui, H. Tan, J. Chen, X. Huang, C. Xu, W. Liu, D.Y.W. Yu, H.H. Hng, H.E. Hoster and Q. Yan; "Cu doped V_2O_5 flowers as cathode material for high-performance lithium ion batteries", *Nanoscale*, Vol. 11, pp. 4937–4943, 2013.
- [13] M. Jiang, S. Bao, X. Cao, Y. Li, S. Li, H. Zhou, H. Luo and P. Jin; "Improved luminous transmittance and diminished yellow color in VO₂ energy efficient smart thin films by Zn doping", *Ceram. Int.*, Vol.40(4), pp. 6331–6334, 2014.
- [14] S.Y. Zhan, C.Z. Wang, K. Nikolowski, H. Ehrenberg, G. Chen and Y.J. Wei; "Electrochemical properties of Cr doped V_2O_5 between 3.8 V and 2.0 V", *Solid State Ionics*, Vol. 180(20), pp.1198 – 1203, 2009.
- [15] A. Bouzidi, N. Benramdane, A. Nakrela, C. Mathieu, B. Khelifa, R. Desfeux and A. D. Costa; "First synthesis of vanadium oxide thin films by spray pyrolysis

- technique", *Mater. Sci. Eng :B*, Vol. 95(2), pp.141–147, 2002.
- [16] D.S. Jung, Y.N. Ko, Y.C. Kang and S.B. Park; "Recent progress in electrode materials produced by spray pyrolysis for next-generation lithium ion batteries", *Adv. Powder Technol.*, Vol. 25(1), pp. 18–31, 2014.
- [17] B.G. Jeyaprakash, K. Kesavan, R.A. kumar, S. Mohan and A. Amalarani; "Temperature dependent grain-size and microstrain of CdO thin films prepared by spray pyrolysis method", *Bull. Mater. Sci.*, Vol. 34, pp. 601–605, 2011.
- [18] R. Irani, S.M. Rozati and S. Beke; "Structural and optical properties of nanostructural V_2O_5 thin films deposited by spray pyrolysis technique: effect of the substrate temperature", *Mater. Chem. Phys.*, Vol. 139(2-3), pp. 489–493, 2013.
- [19] Y. Vijayakumar, G.K. Mani, M.V.R. Reddy and J.B.B. Rayappan; "Nanostructured flower like V_2O_5 thin films and its room temperature sensing characteristics", *Ceram. Int.*, Vol. 41(2), pp. 2221–2227, 2015.
- [20] Z.S.E. Mandouh and M.S. Selim; "Physical properties of vanadium pentoxide sol gel films", *Thin Solid Films*, Vol. 371(1-2), pp. 259–263, 2000.
- [21] Q. Su, W. Lan, Y.Y. Wang and X.Q. Liu; "Structural characterization of β - V_2O_5 films prepared by DC reactive magnetron sputtering", *Appl. Surf. Sci.*, Vol. 255(7), pp. 4177–4179, 2009.
- [22] D.V. Raj, N. Ponpandian, D. Mangalaraj and C. Viswanathan; "Effect of annealing and electrochemical properties of sol-gel dip coated nanocrystalline V_2O_5 thin films", *Mater. Sci. Semicond. Process*, Vol. 16, pp. 256–262, 2013.
- [23] K. Jeyalakshmi, S. Vijayakumar, S. Nagamuthu and G. Muralidharan; "Effect of annealing temperature on the supercapacitor behavior of β - V_2O_5 thin films", *Mater. Res. Bull.*, Vol. 48(2), pp. 760–766, 2013.
- [24] C.M. Muiva, T.S. Sathiaraj and K. Maabong; "Effect of doping concentration on the properties of aluminium doped zinc oxide thin films prepared by spray pyrolysis for transparent electrode applications", *Ceram. Int.*, Vol. 37(2), pp. 555–560, 2011.
- [25] A.L. Patterson; "The Scherrer Formula for X-Ray Particle Size Determination", *Phy. Rev.*, Vol. 56, pp. 978, 1939.
- [26] M. Indumathy, G.K. Mani, P. Shankar and J.B.B. Rayappan; "Effect of nickel doping on structural, optical, electrical and ethanol sensing properties of spray deposited nanostructured ZnO thin films", *Ceram. Int.*, Vol. 40(6), pp. 7993–8001, 2014.
- [27] A. Kumar, P. Singh, N. Kulkarni and D. Kaur; "Structural and optical studies of nanocrystalline V_2O_5 thin films", *Thin solid films*, Vol. 516(6), pp. 912–918, 2008.
- [28] Y. Sun, X. Xiao, G. Xu, G. Dong, G. Chai, H. Zhang, P. Liu, H. Zhu and Y. Zhan;

“Anisotropic vanadium dioxide sculptured thin films with superior thermochromic properties”, *Sci Rep.*, Vol. 3, pp. 2756, 2013.

- [29] M.M.B-Mohagheghi, N. Shahtahmasebi, M.R. Alinejad, A. Youssefi and M. S-Saremi; “The effect of the post-annealing temperature on the nano-structure and energy band gap of SnO₂ semiconducting oxide nano-particles synthesized by polymerizing–complexing sol–gel method”, *Physica B Conde. Matter*, Vol. 403(13), pp. 2431–2437, 2008.
- [30] A.Z. Moshfegh and A. Ignatiev; “Formation and characterization of thin film vanadium oxides: Auger electron spectroscopy, X-ray photoelectron spectroscopy, X-ray diffraction, scanning electron microscopy and optical reflectance studies”, *Thin Solid Films*, Vol. 198(1-2), pp. 251–268, 1991.
- [31] C.V. Ramana, O.M. Hussain, B.S. Naidu and P.J. Reddy; “Spectroscopic characterization of electron-beam evaporated V₂O₅ thin films”, *Thin solid films*, Vol. 305(1-2), pp. 219–226, 1997.